LA-UR- 92-3271

Title: Solutions for Implementing Time-of-Flight Techniques in Low-Angle Neutron Scattering, As Realized on the Low-Q Diffractometer at Los Alamos

LA-UR--92-3271

DE93 003702

Author(s): R. P. Hjelm, Jr., LANSCE
P. A. Seeger, LANSCE

Submitted to: in Proceedings of International Seminar on Structural Investigations of Pulsed Neutron Sources, Joint Institut For Neutron Research, Dubna, Russia

MASTER

Los Alamos
NATIONAL LABORATORY

SOLUTIONS FOR IMPLEMENTING TIME-OF-FLIGHT TECHNIQUES IN LOW-ANGLE NEUTRON SCATTERING, AS REALIZED ON THE LOW-Q DIFFRACTOMETER AT LOS ALAMOS

by

Rex P. Hjelm, Jr and Philip A. Seeger

Los Alamos Neutron Scattering Center

Los Alamos National Laboratory

Los Alamos, New Mexico, 87545-1663

USA

ABSTRACT:

The implementation of small-angle (Low-momentum transfer) neutron scattering instruments at pulsed spallation sources, using time of flight methods, has meant the introduction of some new ideas in instrument design, data acquisition, data reduction and computer management of the experiment and the data. Here we recount some of the salient aspects of solutions for implementing time of fight small-angle neutron scattering instruments at pulsed sources, as realized on the Low-Q Diffractometer LQD, at Los Alamos. We consider, further, some of the problems that are yet to be solved and take a short excursion into the future of SANS instrumentation at pulsed sources.

INTRODUCTION:

The development of pulsed spallation sources as an alternatives to reactors as sources for neutron scattering measurements has increased the availability of neutron scattering instruments for condensed matter research and nuclear physics world wide. The facilities at Rutherford (ISIS) in the UK, Los Alamos (LANSCE) and Argonne (IPNS) National Laboratories in the USA and at KENS in Japan have led to new instrumentation based on the use of time-of-flight (TOF) techniques in various scattering measurements. What concerns us here is the implementation of TOF methods for small-angle neutron scattering at pulsed spallation sources. These have been worth pursuing, as the large demand for small-angle instruments to probe structure in condensed matter at intermediate and long length scales dictates that such machines be built at all available sources. Our efforts have been gra[illegible] the demonstration that SANS inst[illegible] the brightest spallation source, LQ[illegible] at LANSCE, is comparable in many respects with D11 (Seeger and Hjelm, 1991; Hjelm et al 1991)

There are many basic and technical issues that have to be addressed in implementing low-angle instruments on pulsed sources. Some of these are common with instruments at reactors, but others are unique. Many of these have been addressed successfully, and their resolution has been described in a number of publications (Borso et al , 1982; Ishikawa, et al, 1986; Seeger, 1988; Hjelm, 1988; Crawford and Carpenter, 1988, Seeger et al, 1988; Seeger and Hjelm, 1991; Hjelm et al., 1991). Others are still not solved. In this review of our work at Los Alamos we will discuss the general nature of the problems that are overcome in successful use of TOF methods. We will comment on those issues that are currently under development, and in some cases describe our approaches in solving them. Finally, we will take a short look at some of the challenges offered by the development of brighter spallation sources

The challenges in implementing a SANS instrument using TOF methods fall into three classes. The first involves issues associated with the use of a broad neutron spectrum. The second issue concerns the high instantaneous count rates associated with the meas

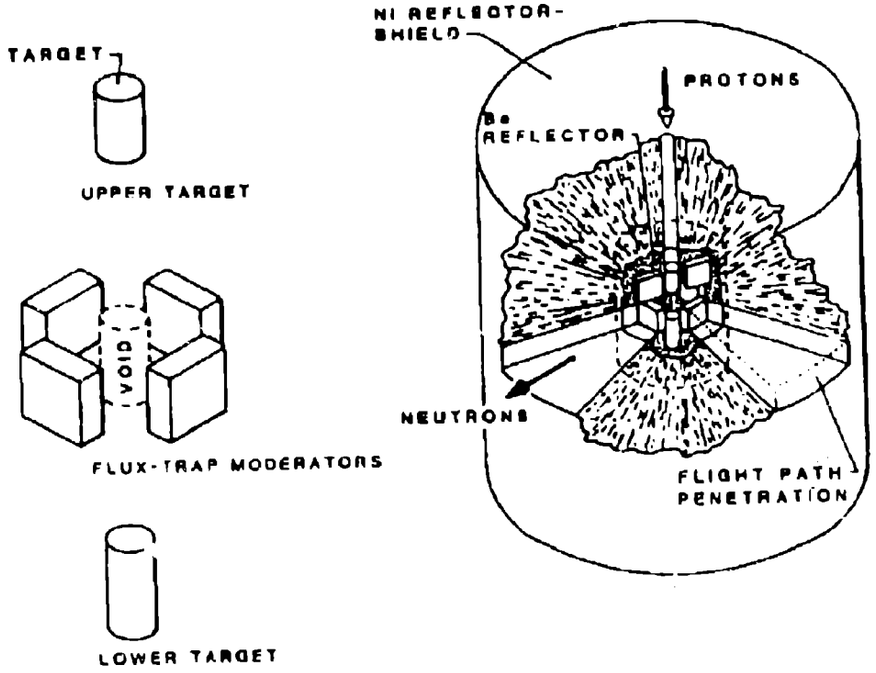

Figure 1: The LANSCE Target, Moderator, Reflector, Shield System: Schematic showing the position of the moderators in the LANSCE target system. The moderators view the flux trap void between the two helves of the split tungsten target.

urement. Finally, the third involves the large histogram size resulting from each measurement, the requirement that the histogram be remapped into meaningful coordinates, and the need to provide the user with a convenient and effective means of dealing with the massive amounts of data present. We will discuss these issues and there solution as we consider the different aspects of the instrument at Los Alamos, the Low-Q Diffractometer, LQD.

SOURCE:

The need to use a broad band neutron beam is a consequence of the fact that at any given wavelength the luminosity, $\Lambda(\lambda)$ (neutrons/Å/sterad/cm^2/s), is low at present pulsed sources. Thus, an integrated wavelength band of neutrons must be employed to obtain reasonable flux, Φ (neutrons/cm^2/s), at the sample; TOF methods are then used to determine the wavelength of each detected neutron. Fortunately, the pulsed nature of the source makes TOF measurements easy. However, the neutrons emerging from the target are not useful as a probe for condensed matter structure: they must be moderated to usable energies. In the small-angle scattering experiment, we are really interested in small momentum transfers, Q. From the relationship between scattering angle, 2θ, and incident neutron wavelength, λ,

$$Q = \left(\frac{4\pi}{\lambda}\right) \sin\theta \cong \frac{4\pi\theta}{\lambda} \qquad 1.$$

where the approximation holds only for small 2θ, we see that low Q is obtained for long wavelengths as well as small-angles. Thus low-Q is best attained using a moderator with higher $\Lambda(\lambda)$ at long wavelengths - a cold moderator.

LQD uses a liquid hydrogen, single phase, cold moderator operated at approximately 23°K and between 4.1 and 12.2 bar. The moderator is situated in flux trap geometry relative to a split tungsten target (Fig. 1, Russell, 1991). The choice of target material in this instance is an important consideration, as fissile materials (eg ^{235}U) give rise to

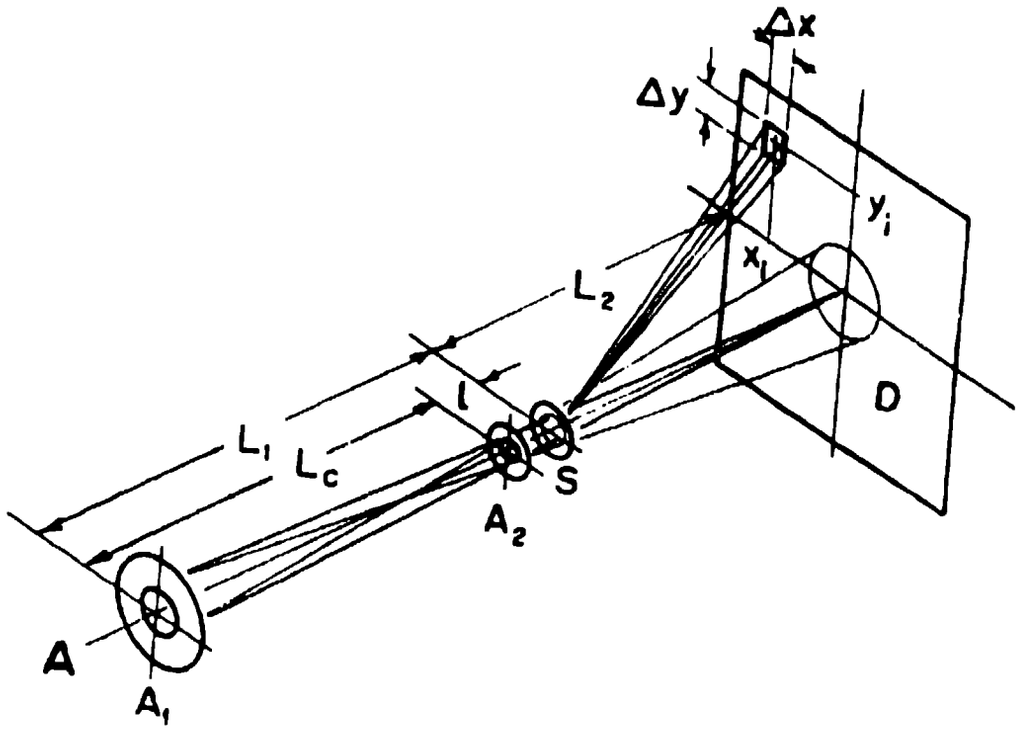

Figure 2. Schematic of a Low-Q Neutron Scattering Instrument with Pin Hole Collimation. Symbols are referred to in the text. A, represents moderator, S, sample, and D, detector.

considerable latent flux that increases the sample dependent background. The use of TOF demands that the time structure of the pulse emerging from the moderator be sufficiently short to allow λ to be determined with precision compatible with the instrument resolution in Q. Thus moderators at pulsed sources tend to be smaller than those at reactors, and the beam is undermoderated. Consequently, in addition to the approximately Maxwellian spectrum, there is substantial flux in the slowing down region of the spectrum going as $1/\lambda$.. The cold moderator at LANSCE has more than sufficient pulse width for the geometric resolution of LQD with maximum width for 15 Å neutrons of 100μs. Other moderator designs with pulse widths up to 300μs are under study. These will afford an increase in $A(\lambda)$ by a factor of three. These involve coupling the cold moderator with the reflector, and premoderation with an ambient temperature water or polyethylene moderator (Watanabe, 1989; Watanabe et al; 1989, Kiyanagi and Wanatabe, 1991).

A consequence of under moderation is a beam containing an epithermal neutron component with energies corresponding to large density of states in the sample. Thus there can be substantial inelastic scatter, leading to sample-dependent background (Hjelm 1988; Seeger and Hjelm, 1991). Further, these neutrons are not well collimated, produce counting rate problems at the detector, and hence, they must be removed. This may be accomplished by a T-zero chopper or with a beam bender. For LQD, we have chosen a highly efficacious and relatively inexpensive method using a filter made of a single crystal of MgO cooled to about 45°K. This method was first used on the SAD instrument at Argonne National Lab. This material has the characteristic of having a sharp scattering edge at roughly 150 meV, and of passing neutrons of lower energy with high transmittance. The filter also removes background γ-radiation emitted from long lived excited stated in the Cd poison layer of the moderator.

COLLIMATION, OPTIMIZATION, AND RESOLUTION:

The direction of the beam momentum is defined by collimation using two pin holes. The collimator geometry is determined by

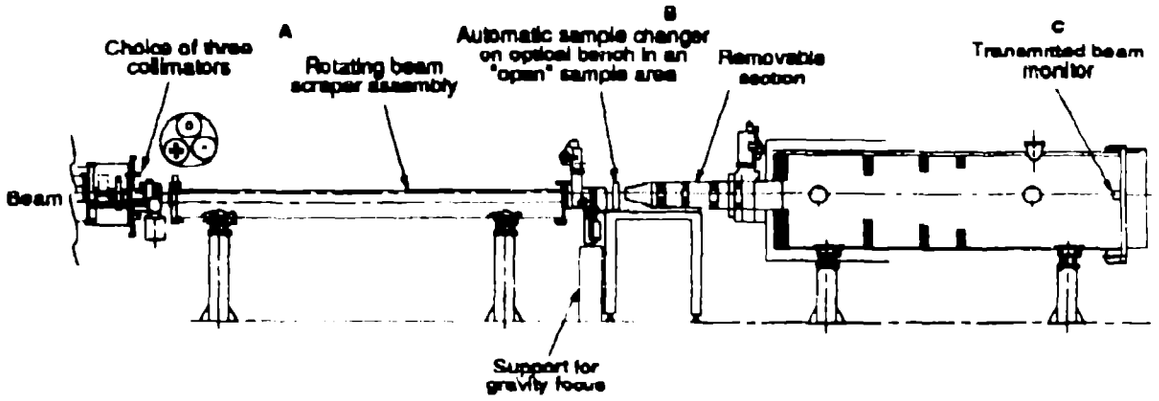

Figure 3. A Plan View of LQD Showing the Basic Elements of the Instrument

optimization of the intensity and resolution (precision in θ). These are related by the usual relationships for pinhole geometry, and assuming isotropic scatter (scalar momentum transfer),

$$\delta I_n = KM\Lambda(\lambda)\Delta\lambda_n A_1 A_2 A_d/(L_1^2 L_2^2) \quad 2.$$

for intensity, δI_n, in the n^{th} time channel, and for the variance in the scattering angle, 2θ in the d^{th} spatial (detector) channel (Schmatz et al, 1976; Seeger, 1980, Mildner and Carpenter, 1984). As shown in Figure 2, the distances along the instrument axis are L_1, the moderator to sample distance, L_2, the sample to detector distance, L_c, the collimator length, and l, the collimator exit aperture to sample position distance. R_1 and R_2 refer to the radii of the collimator entrance and exit apertures, respectively; while Δx_d and Δy_d reference the x and y dimension of the detector element in the d^{th} spatial channel. In our case the locations of events on the area detector (see below) is encoded by calculation of the signal centroid, and V(c) describes the resolution of this.

$$V_d(\theta) = \frac{1}{12}\left[\frac{3R_1^2\left(l+L_2\right)^2 + 3R_2^2\left(L_c+l+L_2\right)^2}{L_c^2 L_2^2} + \frac{\Delta x_d^2 + \Delta y_d^2}{2L_2^2} + V(c)\right] \quad 3$$

The optimization procedure is to minimize V_d while holding δI ([2]) constant, or equivalently to maximize δI while holding V_d constant. We are limited, however, by attainable detector resolution; the next to last term in equation [3] can thus only be made smaller by increasing L_2 and subsequently the total length. In fact the best optimization of count rate and resolution is obtained by lengthening the instrument as much as possible and scaling R_1 and R_2 with the total length. But the total length is also limited, either by the size of the experimental hall, the total solid angle of the moderator as seen from the detector, or (for a pulsed source) by the "frame overlap" condition of fast neutrons from a subsequent pulse catching up with the slow, long wavelength neutrons. In low-Q the latter are important as discussed in equation [1]; thus this situation must be avoided. A further complication of the optimization for a pulsed source is the spectrum of incident neutron wavelengths; as L_2 is varied, a given Q-value occurs at the same place on the detector at a different λ. Optimization leads to placing the moderator as close as possible to the collimator, and likewise the sample. For a pulsed source, where there is a cut off in the incident beam spectrum, and as a consequence of optimization in Q involving simultaneous optimization over a range of θ, optimization approaches the case where L_1 and L_2 are equal. Finally the aper-

ture and detector element sizes should be related such that $R_1 = 2R_2 = (1/3)^{1/2} \Delta x_d = (1/3)^{1/2} \Delta y_d$. L_2 is fixed to the aperture radii in this scheme by the requirement that the beam umbra be focused to a point at the detector (Fig. 2). These rules are implemented as much as practical; some limitations as the total length of the instrument is fixed by factors listed above, commercial detectors are used (consequently Δx and Δy are fixed), and that space is needed between the moderator and collimator to place a shutter, beam filter and/or chopper(s). Intensity at the detector can be increased by increasing the number of collimator apertures, M, in equation [2]., without sacrificing resolution. Provision is made for multiple pin holes (Fig. 3) with intermediate baffles to prevent cross talk (Seeger et al 1990).

There is a problem with collimation and the neutron trajectories. Over the total length of the instrument the neutron falls under the force of gravity; the slower neutrons fall the greater distance. This results in substantial loss in resolution in the vertical direction of the machine (Bothroyd, 1989). The solution is to use a moving aperture at the collimator exit that is accelerated upward at a constant rate during the course of a TOF frame to select those neutrons with the trajectory that hits the center of the detector (the beam stop). Such a device has been implemented on LQD (Fig. 3; Seeger et al, 1990). It is activated hydraulically; though other designs, activated mechanically by cams, say, are being considered.

SAMPLE AREA:

The sample area of the instrument is designed to be highly flexible and to take a variety of sample holders and instrumentation with a minimum amount of time, and hence, lost beam. This is driven by the fact that small angle instruments are used for more different types of science, samples and conditions than any other type of neutron scattering instrument. The sample area is "open"; the flight path vacuum is simply interrupted at the sample position to enable easy access (Fig. 3). Fused silica windows are used to contain the vacuum of the primary and secondary flight paths. Short sections of the secondary flight path can be removed to provide different gap lengths (up to 1 m) along the flight path. Very large apparatus can be installed by removing a roof on the instrument enclosure. In the standard configuration the sample apparatus is mounted on an optical bench, and standard types of positioners and holders are used. Sample alignment is made easy by the use of an alignment telescope that views the sample from the detector position, down the optical axis of the instrument by means of a mirror that is inserted directly in front of the detector. A surveyor's target mounted on the downstream side of the incident beam monitor serves as one reference point, with the exit aperture of the collimator serving as the other.

DETECTOR:

The detector on LQD is a Rösø ^{3}He, two dimensional position sensitive proportional counter. It is here that we see our most serious unsolved problem in the use of TOF techniques for SANS. The peak of the moderated spectrum involves high instantaneous counting rates that create considerable misencoding and dead time problems. This problem will only become more severe as brighter sources become available. This issue must be resolved through the development of faster detectors, detector electronics and encoding schemes. Some effort has been made in this area using scintillation counters, but the use of these detectors is hindered by sensitivity to γ radiation.

Because of the wide dynamic range afforded by the TOF technique, the detector can be fixed in position. Thus the collimation can be optimized with respect to both intensity and Q precision. Further, baffles can be installed in scattering flight path tube to reduce back grounds (Fig. 3).

DATA ACQUISITION:

The data acquisition system consists of several Fastbus modules (Fig. 4; Nelson et al 1985; Poore et al 1985). The spatial and TOF channels from the detector are mapped into a histogramming memory consisting of two modules, each having a capacity of 2×10^6 24 bit words. The mapper can work at a peak

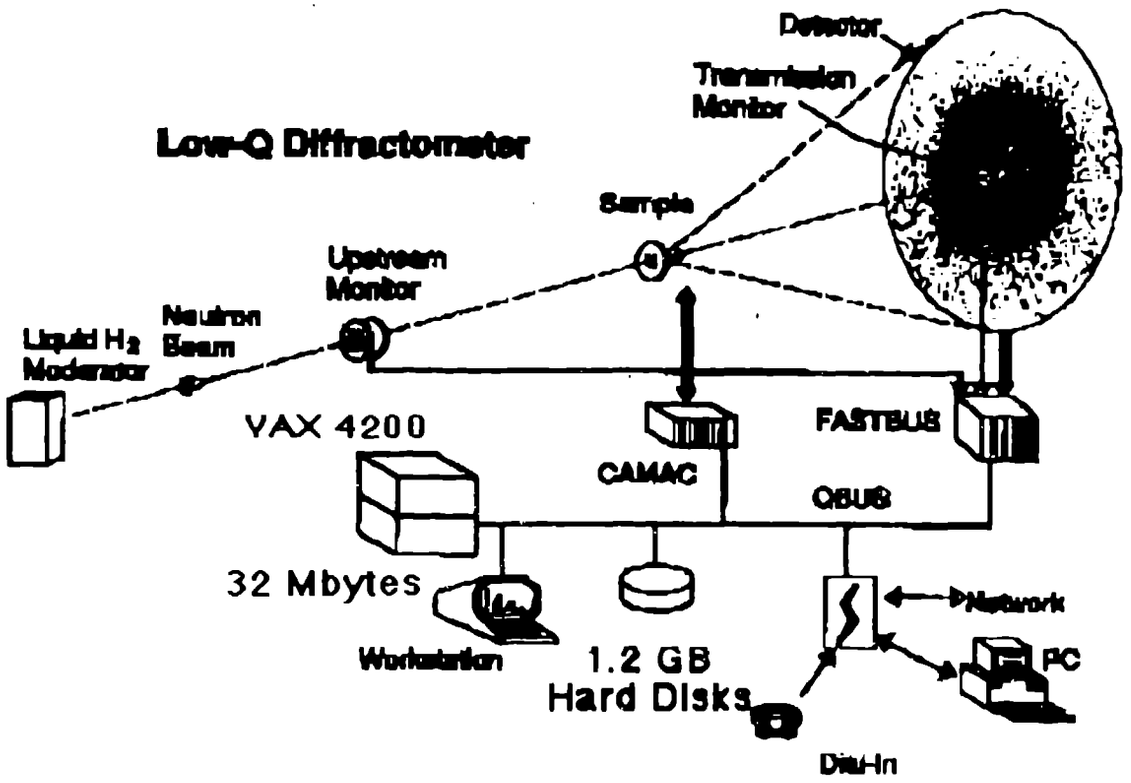

Figure 4. A Schematic of LQD, Data Acquisition and Computer Systems.

rate of 600 KHz. This gives considerable latitude for implementing "smart" programmable mappers without the necessity of inserting a computer into the data acquisition path. We currently take data in 128x128 spatial channels and 197 time channels. These numbers correspond to sampling counts at 0.307 cm intervals in x and y. The TOF channels are "logarithmic", having constant $\Delta t/t$ of 0.016, where t is TOF time. The three dimensional histograms are thus large, containing in excess of 3 Megawords in our present configuration. This creates substantial burdens on the computational abilities.

Data transfer is directly out of Fastbus histogram memory and onto a hard disk, under the control of a VAX-4200 cpu, currently configured with 32 mbyte memory and 1.2 Gbyte in hard disk (Fig 4). This processes is speeded considerably by direct streaming of the data onto a dedicated part of the hard disk, and currently takes about 85 seconds for 9 Mbytes. This file is then compressed in a background process on the LQD VAX. Typically, compression is made by about a factor of 10 to 11 and takes 90 seconds of CPU time. It takes 45 seconds to clear the Fastbus histogram plus about 20 to 30 seconds of overhead, so the minimum time between the end of one run and starting the next is 2.5 minutes. The time between saves is about 3.5 minutes, which defines the maximum rate that samples presently can be put through the instrument. With the likely advent of brighter sources, we would like to improve this figure significantly to enable new types (kinetic and dynamic, for example) of measurements.

The LQD computer is networked to other instrument-dedicated VAXen and two VAX 4500 boot nodes. The boot nodes are used in data reduction tasks, about which we will have more to say below. This network of instrument VAXen is further clustered with other networks at LANSCE to make approximately 50 machines in the LANSCE system. These are also networked to Macintoshes and PC's that are available throughout LANSCE. The compressed data files are permanently archived on a jukebox WORM drive with a total capacity of 0.32 Terabytes. A VAX is dedicated to managing this drive for data

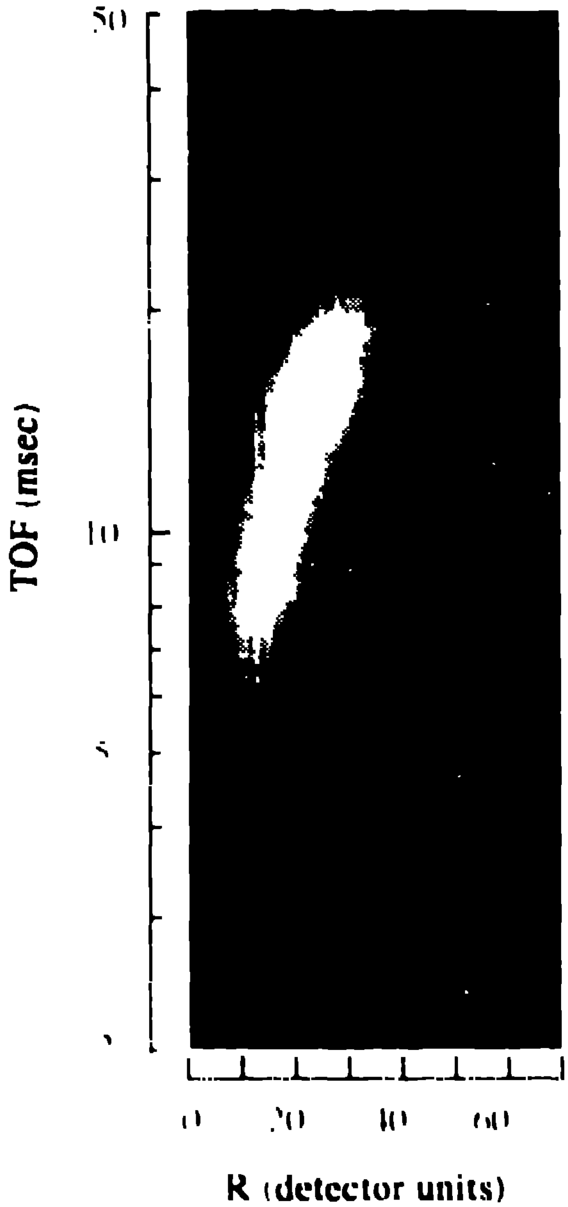

[illegible] The [illegible] indicates [illegible] highest [illegible] brightness.

[illegible] storage and retrieval for [illegible] data [illegible] at LANSCE.

One might think with such a high capacity in computational power that this system would not be a bottleneck in the effective use of an instrument [illegible] TOF method. If we were [illegible] only with taking data and were [illegible] with a rather leisurely pace in data [illegible] and analysis, this would be [illegible]. However, [illegible] must be able to assess the [illegible] data which [illegible] been taken [illegible] every [illegible] thereafter. This means [illegible] data must be [illegible]

reduced, properly normalized and corrected within a time span of less than a few minutes. Even more decision making power can be handed to the experimentalist if past examples can be likewise processed for comparison. These issues are important for a large [illegible] ized user facility, as all pulsed sources are. The user's opportunity to conduct measurements is limited to a few days, at most, and it may be months or a year before the next opportunity. He or she must be given every chance to do it right the first time.

Servicing this requirement [illegible] highly advanced computer system [illegible] mention the highly dedicated instrument scientists at LANSCE, and, farther [illegible] extensive software development. The [illegible] for TOF SANS stem not only from the [illegible] of the data sets, but also from the [illegible] which measurements are made [illegible] averages per 30 minutes beam time [illegible] LANSCE operating at 60 µA proton [illegible] on target, and this number will only increase with a brighter source. Thus data throughput in this system is very large and will grow larger. Further, users are only at the facility for a couple of days, at least in the [illegible] a low angle instrument. Thus the [illegible] must be fairly easy to use and [illegible]. This is all the more important as the [illegible] tion procedure can be done [illegible] ways, and the best [illegible] for a particular measurement at [illegible] be readily apparent. The software [illegible] [illegible] research tool [illegible]

DATA REDUCTION

One of the most important [illegible] have to be addressed [illegible] TOF [illegible] mapping of [illegible] into [illegible] Figure [illegible] shows an example of [illegible] from a [illegible] sample [illegible] TOF radially averaged R [illegible] seen the characteristic scattering peak [illegible] distorted [illegible] beam spectrum and [illegible] R [illegible] Q [illegible]

master equation for mapping, in absolute differential scattering probability, is

$$dP(Q_k)/d\Omega = \frac{\sum_{\{d,n\}=k} N_{d,n}}{\sum_{\{d,n\}=k} \Phi_n \Omega_d} \qquad 4.$$

where we specify the sum to be over that set of time n, and spatial, d, channels that contribute to the k^{th} Q bin according to the relation $Q_k = 4\pi/\lambda_n \sin\theta_d$. The form of equation [3] derives from the consideration that the counts in any d,n cell, $N_{d,n}$ must be weighted by the number of counts in that could have been measured in that cell, $\Phi_n \Delta\Omega_d$ in order to optimize the information content in Q from the counts in each cell (Seeger and Pynn, 1986; Hjelm 1987, Hjelm 1988; Seeger and Hjelm, 1991). Normalization is then given by a similar sum of products of measured transmitted beam in each time channel, Φ_n, with the solid angle subtended by the spatial channel, $\Delta\Omega_d$. All relevant corrections, such as detector non linearity (Seeger and Hjelm, 1991), are made to $N_{n,d}$ before summing. Equation [4] implies very careful measurement of Φ properly normalized for $\Lambda(\lambda)$ by comparison with some scatterer of known $dP/d\Omega$ (Jacrot and Zaccai, 1981; Wignal and Bates, 1987). Conversion of $dP/d\Omega$ to the more usual macroscopic differential cross section per unit scattering volume, $d\Sigma(Q)/d\Omega$ (cm^{-1}), is made by dividing equation [4] by the sample path length. The propagation of errors defining the uncertainties in $dP/d\Omega$ is straightforward using the usual methods, but *must* be done at every step in parallel with the corrections and normalizations.

Each n,d cell caries with it different information on $dP/d\Omega$ and on Q. We have already discussed the former. The contribution of each cell to the variance in Q is

$$V_{n,d}(Q) = Q^2_{n,d}\left[\frac{V_d(\theta)}{\theta^2_d} + \frac{V_n(t)}{\bar{t}^2_n}\right] \qquad 5.$$

where the averages over n,k cell and d and n channels are indicated by the bar. The variance of the time values in the n^{th} channel is $V_n(t)$, and $V_d(\theta)$ is given by equation [3]. Equation [5] shows why the "logarithmic" TOF binning scheme is preferred in data acquisition, as $V_n(t)/\bar{t}^2_n = \frac{1}{12}(\Delta t/t)^2$ constant, which can be set to match the smallest value of the first term in equation [5]. This is the only means by which the two parts of the instrument resolution can be matched in a TOF-SANS measurement.

The precision in Q in each bin as a consequence of combining cells is calculated using the relation

$$V_k(Q) = \overline{V_{\{n,d\}=k}(Q)} + V\left(\overline{Q_{\{n,d\}=k}}\right) \qquad 6.$$

which means that the variance of the k^{th} Q bin is the sum of the average variances of the n,d cells (given in each case by equation [5]) in the bin and the variance of the average Q's of these cells. We combine the cells according to the weighting discussed in introducing equation [4]. Thus the information content in $dP/d\Omega$ is coupled with that in Q, and

$$V_k(Q) = \frac{\sum_{\{n,d\}=k} N_{n,d} V_{n,d}(Q)}{\sum_{\{n,d\}=k} N_{n,d}} + \left[\frac{\sum_{\{n,d\}=k} N_{n,d}\overline{Q_{n,d}}}{\sum_{\{n,d\}=k} N_{n,d}}\right]^2 \qquad 7.$$

Equation [7] implies an additional weighting factor in the mapping, as one may wish to exclude cells whose contribution to the total variance is excessive when compared to the variance from the Q-bin width. Thus a selection criterion is used

$$V_{n,d}(Q) < \frac{f}{12}\Delta Q^2_k \qquad 8.$$

to determine whether a cell should be used in the mapping, where f is some number relating the maximum cell variance to the Q bin variance. Usually we chose $f = 1.5$. Equations [4] through [7] imply further that the size of

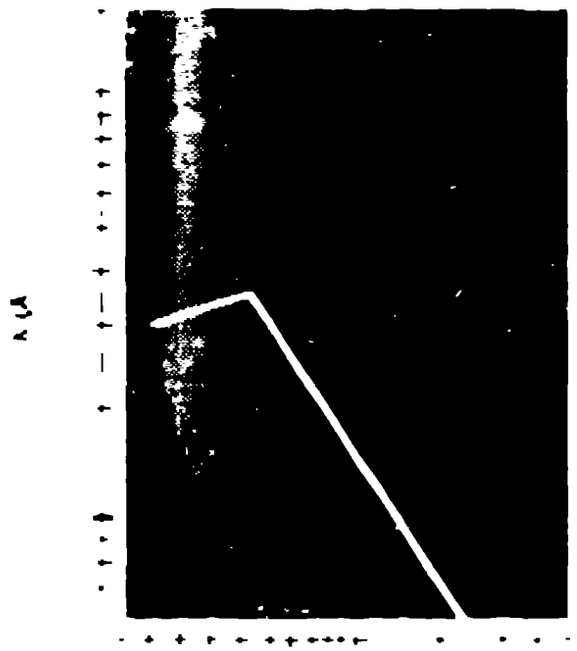

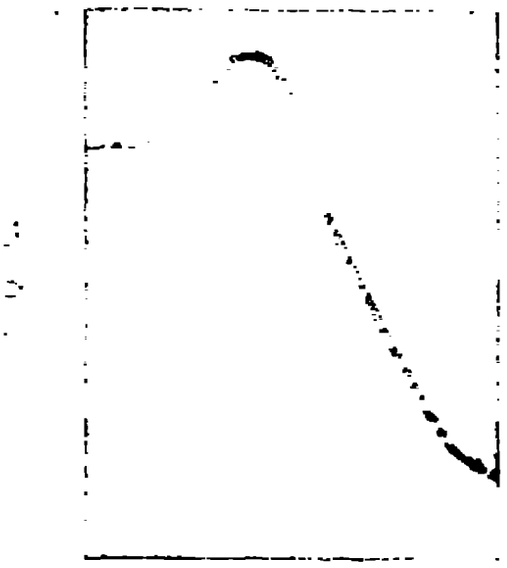

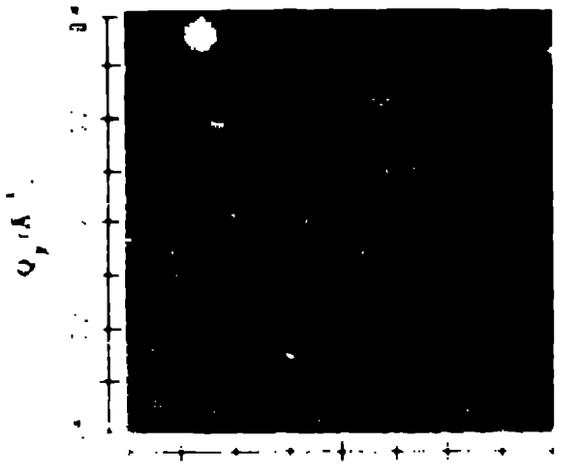

THE USER
INTERFACE SOFTWARE

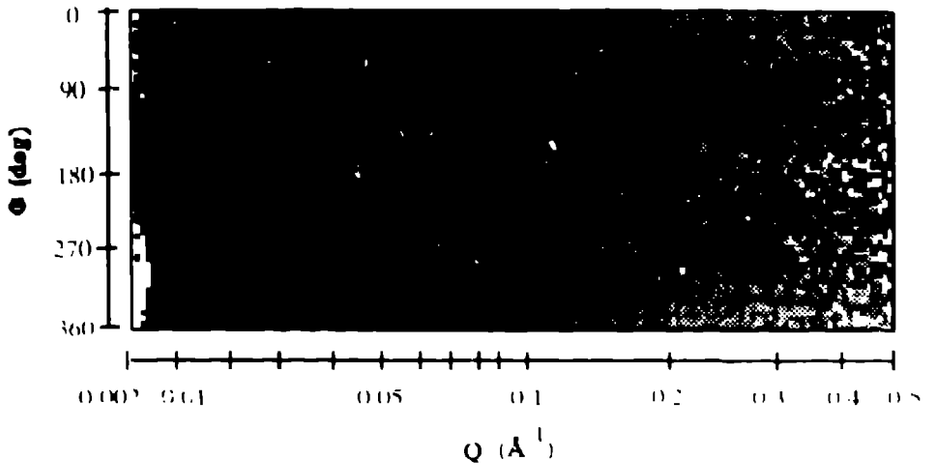

Figure 9. dP/dΩ mapped into Φ,Q for the Smectic A Phase of a Liquid Crystal Polymer. The smae data shown in Fig. 8. Data is displayed in negative contrast.

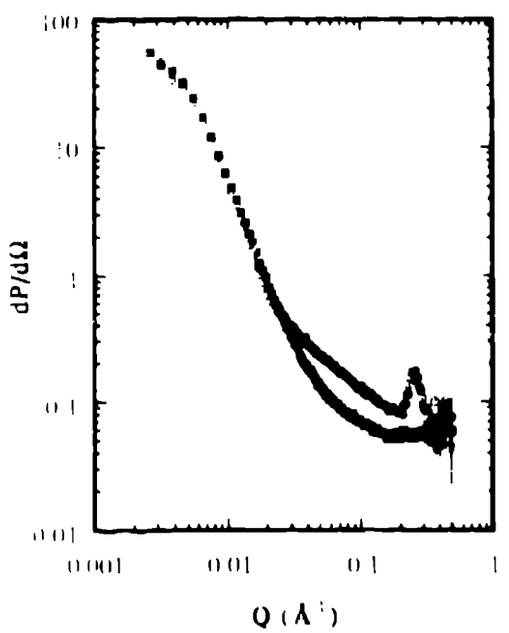

Figure 10. Sector Averages of dP/dΩ for a Liquid Crystal Polymer in the Smectic A Phase. Data from Figs. 8 and 9. ○, averaged across a sector in the y direction. ■, averaged across a sector in the x direction.

directed in directions of interest. These segments are defined by a masking function. In each case the rms errors of the result, in both Q and dP/dΩ, are carried through. These are displayed in the scalar Q maps, and are retained as separate maps in the vector maps. All files output from SMR contain the map and the rms error in dP/dΩ, and all one dimensional files also include the rms of the distribution on Q in each bin (Fig 10). Near real-time maps are currently made by selecting very narrow time slices covering a Q-range of immediate interest, and mapping this. SMR also performs a limited number of SANS data analyses (eg Guinier analysis) for quick assessment purposes. A second program, EZP, is used for more extensive SANS data analysis, as well as user defined analysis. This program also features some basic interactive graphics capabilities. Many of the features of EZP are also available in a series of programs written in FORTRAN 77 for transportability to other computers (eg PC's or Mac's). Standard SANS analysis tools are part of this package. These programs all rely on a standard ASCII file format described in an earlier publication (Hjelm and Seeger, 1989). Output in other recognized formats are available for our users who may have software written for these types of files. We are currently developing other programs and interfaces to ease the transfer of reduced data to PC's and Macintosh's (in fact Figs. 9 & 10 were composed on the Macintosh using these programs). This opens to the user the exceptional power in data display and analysis of the graphics software available on these platforms.

THE FUTURE—NEW SOURCES, NEW PROMISES, NEW CHALLENGES:

Proposals for the development of new spallation sources operating in the 1-5 MW range (LANSCE presently operates at 50-80 kW) offer exceptional promise and opportunity for neutron scattering at pulsed sources. They also present some important challenges. The larger fluxes at long wavelengths from these sources will enable instruments that will go to lower Q than presently practical on pulsed sources. We will need to learn how to build such instruments and over come the difficulties with collimating long wavelength neutrons to meet the demand to probe longer length scales in condensed matter research. .The development of new detectors that can handle the extremely large instantaneous data rates anticipated for these new sources is a prime challenge. Given this development, experiment turnover and data through put will be even faster, maybe by an order of magnitude, than those on even the brightest spallation source available today. This will place ever increasing demand on computers and computer software. Faster machines will be available, to be sure, but software development will have to be even more user friendly and self documenting if the user is to make full use of the potential of our new instruments. Fortunately, we are likely to have help in these issues, as new developments in computers are tending toward common vendor standards that allow applications to communicate with one another. Using these a building blocks along with the new windows environments that are emerging, one can envision constructing highly complex. portable systems, which will meet the demands of a new era.

ACKNOWLEDGEMENTS :

The authors whish to thank Dr Satyen Kumar and Mr. Joe Mang for permission to include there data on liquid crystal polymers. This work benefited from the use of the Low-Q Diffractometers at the Manuel Lujan Neutron Scattering Center of the Los Alamos National Laboratory which is supported by the Office of Basic Energy Sciences of the United States Department of Energy under contract W-7405-ENG-36 to the University of California.

REFERENCES:

Boothroyd, A.T. (1989), *J. Appl. Cryst.*, **22**, 252-255.

Crawford, R.K., and Carpenter, J.M. (1988), *J. Appl. Cryst., 21, 589-601.*

Ghosh, R.E. and Rennie (1990), *Conferences in Physics*, **100**,

Hjelm, R.P. (1987), *J. Appli. Cryst..*, **20**, 273-279.

Hjelm, R.P. (1988), *J. Appl. Cryst..*, **21**, 618-628.

Hjelm, R.P., and Seeger, P.A. (1989) *Conferences in Physics*, **97**, 367-387.

Hjelm, R.P, Seeger, P.A., and Thiyagarajan, P. (1991), *Proceedings of the 11th Meeting of the International Collaboration on Advanced Neutron Sources*, October 22 - 26, Tskuba, Japan. KEK Report 90-25, 673-676.

Ishikara, Y., Furusaka, M., Nimura, N, Arai, M. and Haaegawa, K. (1986), *J. Appl. Cryst.*, **19**, 229-242.

Jacrot, B., and Zaccai, G. (1981) *Biopolymers*, **20**, 2413-2426.

Kiyanagi, Y. and Wanatabe, N, (1991), *Proceedings of the 11th Meeting of the International Collaboration on Advanced Neutron Sources*, October 22-26, 1990, Tskuba, Japan. KEK Report 90-25, 408-414.

Mildner, D.F.R. and Carpenter, J.M. (1984), *J. Appl. Cryst.*, **17**, 249-256.

Mildner, D.F.R. and Carpenter, J.M. (1987), *J. Appl. Cryst.*, **20**, 419-424.

Nelson, R.O., Burrus, D.M., Cort, G., Goldstone, J., McMillan, D.E., Poore, R.V. (1985), *IEEE Trans.. Nucl. Sci.*, **Ns-32**, 1422.

Poore, R.V., Burrus, D.M., Cort, G., Goldstone, J.A., Miller, L., and Nelson, R.O. (1985), *IEEE Trans.. Nucl. Sci.*, **Ns-32**, 1290.

Russell, G.J. (1991), *Proceedings of the 11th Meeting of the International Collaboration on Advanced Neutron Sources*, October 22 - 26, Tskuba, Japan. KEK Report 90-25, .335-339.

Schmatz, W., Springer, T., Schelten, J., and Ibel, K (1974). *J. Appl. Cryst.*, 7, 96-116.Seeger, P.A. (1980), *Nucl. Instrum. Methods*, **178**, 157-161.

Seeger, P.A., and Pynn, R. (1986), *Nucl. Instrum. Methods*, **A245**, 115-124.

Seeger, P.A., and Hjelm, R.P. (1991), *J. Appl. Cryst.*, **24**, 467-478.

Seeger, P., Hjelm, R.P. and Nutter, M. (1990),*Molecular Crystals Liquid Crystals*, **180A**, 101-117.

Watanabe, N (1989), *Conferences in Physics*, **97**, 763-769.

Watanabe, N., Kiyanagi, Y., Inoue, K., Furusaka, M., Ikeda, S., Arai, M., Iwasa, H. (1989), *Conferences in Physics*, **97**, 787-797.

Wignal, G.D. and Bates, F.S. (1987), *J. Appl. Cryst.*, **20**, 28-40.